Polymer 50 (2009) 2544–2550

Contents lists available at ScienceDirect

Polymer

journal homepage: www.elsevier.com/locate/polymer

Preparation and properties of organic–inorganic hybrids based on poly(methyl methacrylate) and sol–gel polymerized 3-glycidyloxypropyltrimethoxysilane

Marica Ivanković [a,*], Ivan Brnardić [a], Hrvoje Ivanković [a], Miroslav Huskić [b], Andreja Gajović [c]

[a] University of Zagreb, Faculty of Chemical Engineering and Technology, Marulićev trg 19, P.O. Box 177, HR-10001 Zagreb, Croatia
[b] National Institute of Chemistry, P.O. Box 660, 1001 Ljubljana, Slovenia
[c] Ruđer Bošković Institute, Bijenička 54, P.O. Box 180, HR-10002 Zagreb, Croatia

ARTICLE INFO

Article history:
Received 10 October 2008
Received in revised form
10 March 2009
Accepted 23 March 2009
Available online 21 April 2009

Keywords:
Organic–inorganic hybrids
PMMA
Sol–gel

ABSTRACT

New organic–inorganic hybrid materials were prepared by the sol–gel process. Simultaneous polymerizations of methyl methacrylate (MMA) and an organically modified silicon alkoxide, 3-glycidyl oxypropyltrimethoxysilane (GLYMO), with varying MMA/GLYMO molar ratios, were performed. Poly (oxypropylene)diamine was used as an epoxy opening agent, as basic catalyst for GLYMO condensation and as poly(methyl methacrylate) (PMMA) crosslinking agent. Chemical reactions and the structure of prepared hybrids were studied by means of Fourier transform infrared (FTIR) spectroscopy, nuclear magnetic resonance (NMR), differential scanning calorimetry (DSC), thermogravimetric analysis (TGA), dynamic mechanical analysis (DMA) and by scanning electron microscopy (SEM). Depending on the ratios of organic and inorganic components hybrids showed either a discrete microstructure or interpenetrating polymer network (IPN) structure. Silsesquioxane (SSQO) structures formed as a result of GLYMO hydrolysis and condensation in the sol–gel process influence the glass-transition temperature of PMMA. The hybrids have much better thermal stability than PMMA, their surfaces are more hydrophilic than PMMA and they may have potential as damping materials.

1. Introduction

In the last decade, organic–inorganic hybrids became a fascinating new field of research. One of the main reasons for this is the chance of obtaining the desired and sometimes unique end properties, which can be hardly reached if only organic or inorganic components are used [1]. Small amounts (several wt%) of nanometer-sized particles in polymer matrices can considerably influence mechanical, optical, heat-resistant, and other properties of these systems. One of the most common ways for nanoparticle preparation is the sol–gel process [2–10]. The inorganic nanostructures can either be formed *in situ* simultaneously with organic polymer or they can be first prepared and then added to polymerizable monomers or to polymer solution. The presence of covalent bonding between organic and inorganic components reinforces interaction between components and improves the properties of hybrid materials [9].

One of the widely studied hybrid systems is based on SiO_2 and poly(methyl methacrylate), PMMA. The hydrolysis and condensation (sol–gel process) of tetraethoxysilane, as a silica source, has widely been used [11–17].

Polyhedral oligomeric silsesquioxanes (POSS) of nanosized cage-like structures with a formula of $(RSiO_{3/2})_n$ (where $n = 6, 8, 10\ldots$ and R is an organic group), and POSS containing polymers were also blended with PMMA [18–23].

Less work has been reported on organic–inorganic hybrids based on PMMA and *in situ* formed silsesquioxane (SSQO) structures, as a result of the sol–gel polymerization of trialkoxysilanes, $RSi(OR')_3$.

In the present study, we report on the synthesis and properties of organic–inorganic hybrids based on PMMA and sol–gel polymerized 3-glycidyloxypropyltrimethoxysilane (GLYMO). Poly(oxypropylene)diamine was used as an epoxy opening agent, as basic catalyst for GLYMO condensation and as PMMA crosslinking agent. In all investigated systems a non-stoichiometric NH/epoxy ratio, *r*, was 4.

3-Glycidyloxypropyltrimethoxysilane is one of the most popular sol–gel precursors. It is a trialkoxysilane with a short hydrocarbon chain bearing an epoxy functional group:

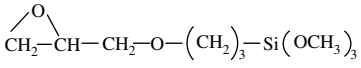

GLYMO can undergo a variety of reactions during the preparation of a hybrid by the sol–gel process. Hydrolysis of the methoxy groups gives silanol groups which can subsequently condense to form the silsesquioxane structures [24].

* Corresponding author. Tel.: +385 1 4597 230; fax: +385 1 4597 250.
E-mail address: mivank@fkit.hr (M. Ivanković).

0032-3861/$ – see front matter © 2009 Elsevier Ltd. All rights reserved.
doi:10.1016/j.polymer.2009.03.059

The sol–gel polymerization of GLYMO depends on the catalysis, solvent, amount of water used, and temperature. It is well known that under acid catalysis, loose, coil-like SSQO structures are formed, whereas basic catalysts promote fast polycondensation leading to compact, cage-like products [25].

Low-temperature epoxy ring opening in GLYMO can be achieved by the use of amine curing agent such as poly(oxypropylene)diamine, well known under the trade name Jeffamine (e.g. D230):

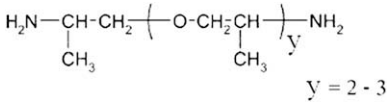

In principle each active hydrogen in the amino group is capable of opening and linking to one epoxy group. Since the amines are basic, they also catalyse the condensation of silanol groups to form the silsesquioxane structures.

Apart from the mentioned reactions, aminolysis of PMMA ester groups and crosslinking of PMMA [26,27] with D230 and SSQO-D230 structures is also possible.

Our interest in this work was the preparation of SSQO-containing hybrid networks by *in situ* bulk polymerization. It was expected that prepared materials could provide favorable combination of properties from inorganic structures and organic polymers. Chemical reactions and the structure of prepared hybrids were studied by means of Fourier transform infrared (FTIR) spectroscopy, nuclear magnetic resonance (NMR), differential scanning calorimetry (DSC), thermogravimetric analysis (TGA), dynamic mechanical analysis (DMA) and by scanning electron microscopy (SEM).

2. Experimental

2.1. Materials

Methyl methacrylate, MMA (Rohm and Haas Co., Germany), monomer was purified by distillation under reduced pressure. Azobisisobutyronitrile, AIBN (AKZO Chemie, The Netherlands), was recrystallized repeatedly from cold methanol and dried in a vacuum oven. 3-Glycidyloxypropyltrimethoxysilane, GLYMO (98%), was supplied by Aldrich Chemicals and poly(oxypropylene)diamine, with an average molecular weight of about 230, was provided under the trade name Jeffamine D230 (in further text D230) by Fluka (Buchs, Switzerland). The latter materials were used as received.

2.2. Preparation of the organic–inorganic hybrids

Prior to the preparation of the organic–inorganic systems there were a number of preliminary studies which are worth noting [28]. Separately, the polymerization of MMA, the inorganic polymerization of GLYMO by sol–gel process (hydrolysis and condensation reactions), as well as reactions in the systems MMA/D230 and GLYMO/D230 were studied. Based on the aforementioned preliminary studies [28] the detailed procedure of synthesis of organic–inorganic hybrids can be described as follows.

An aqueous solution of acetic acid, AA, was added to GLYMO employing a molar ratio GLYMO:H_2O:AA = 1:1.5:0.01. This solution was stirred at room temperature for 1 h then mixed with D230 (molar ratio GLYMO:D230 = 1:1) and stirred for another 30 min. Various amounts of MMA were then added to the solution and stirred for 1 h. Molar ratio MMA:GLYMO was 15:1 (sample H3); 7:1 (sample H5); 3.6:1 (sample H7) and 1.7:1 (sample H9). Numbers in the sample designations represent approximate weight percent of inorganic phase calculated as $SiO_{1.5}$. AIBN was used as initiator of MMA polymerization. The mixtures were left for 24 h at room temperature in the flat-bottomed flask equipped with a reflux condenser and a nitrogen inlet. The viscous liquids were placed between two glass plates with a rubber spacer which allowed to prepare polymer sheets approximately 2 mm thickness. The samples were then cured at 65 °C for 24 h and post-cured at 140 °C for 12 h.

2.3. Characterization

The infrared spectra of investigated materials were recorded by a Fourier transform infrared (FTIR) spectrometer (Bruker Vertex 70) equipped with an attenuated total reflection (ATR) accessory with a diamond crystal. Sixteen scans were collected for each measurement over the spectral range of 400–4000 cm^{-1} with a resolution of 4 cm^{-1}.

^{29}Si CP MAS spectra were recorded with Varian Unity Inova 300 MHz NMR spectrometer at 60.19 MHz. Contact time was 5 ms, delay time 2 s, acquisition time 100 ms, spin rate 5000 Hz, and number of scans 9–40,000.

Glass-transition temperature of PMMA and hybrids was determined by differential scanning calorimetry (DSC) using a Netzsch DSC 200 equipped with a liquid nitrogen cooling accessory. The heating rate was 10 °C min^{-1}.

The DMA measurements were carried out on a DuPont TA Instruments DMA 983 using rectangular samples ($60 \times 10 \times 2 \pm 0.5$ mm^3) at a constant oscillation frequency of 1 Hz and heating rate of 2 °C min^{-1}. The range of temperature was −120 °C to 180 °C and the displacement amplitude was 0.2 mm.

Fracture surface of cured specimens after tensile tests at room temperature was studied by scanning electron microscope JEOL T300 operated at 25 kV. The samples were gold-coated.

Contact angles of PMMA and hybrid surface with water, diiodomethane and formamide were measured with DataPhysics OCA-20 (DataPhysics Instruments GmbH, Filderstadt, Germany) in a stationary mode. At least five measurements of angles were recorded and the results quoted are an average. The surface-free energy (γ) and its dispersive (γ^d) and polar components (γ^p) were estimated using the harmonic mean method proposed by Wu [29].

Thermogravimetric analysis (TGA) was performed on a Perkin Elmer thermobalance TGS-2. Samples weighing ~15 mg were heated from room temperature to 1000 °C at heating rate of 10 °C min^{-1} in a synthetic air or nitrogen flow of 150 cm^3 min^{-1}.

Tetrahydrofuran (THF) extractions of samples were performed for 3 days to determine the fraction of gel. THF was changed every day for a pure charge. After the extraction, the samples were dried in vacuum at 100 °C till weight constancy. The fraction of gel was determined as the ratio of the mass of the dry sample after extraction and its mass before extraction.

3. Results and discussion

3.1. FTIR spectroscopy

The FTIR spectra of investigated systems are shown in Fig. 1(a) and (b). The FTIR spectrum of PMMA shows the characteristic carbonyl vibration absorption of ester side group at ~1720 cm^{-1}. Polymerization of methyl methacrylate in hybrid systems was evidenced by the disappearance of the stretching vibration bands of the vinyl group at 1639 cm^{-1}.

To prove the covalent bonding between PMMA and D230 the insoluble part of the sample (after solvent extraction) was used for the FTIR measurement. As seen from Fig. 1(a), several peaks in the 1500–1700 cm^{-1} region as well as a broad peak between 3100 and 3600 cm^{-1} appeared. The peak at ~1665 cm^{-1} is assigned to the amide C=O stretching vibration while the peaks at ~1580 cm^{-1} and 1510 cm^{-1} are characteristic of the amide C–N stretching vibration and the in-plane N–H bending, respectively. A broad band between 3100 and 3600 cm^{-1} is assigned to the amide N–H stretching vibration.

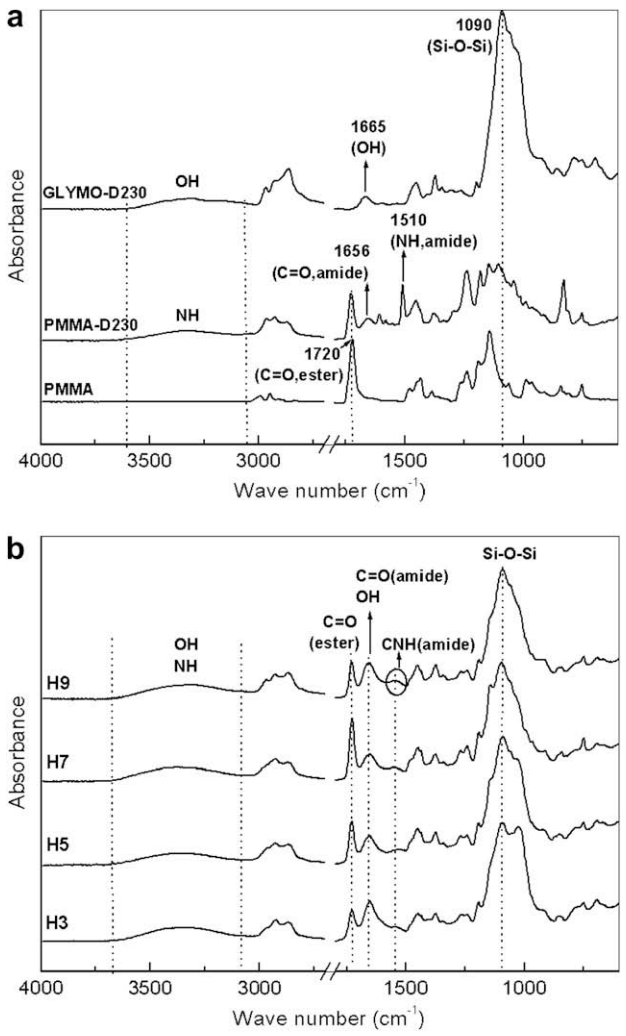

Fig. 1. FTIR absorption spectra of investigated system.

In the FTIR spectrum of GLYMO–D230 the intensities of peaks related to epoxide ring at 1254, 909 and 850 cm^{-1} seemed to have decreased or even disappeared but it is difficult to determine if the epoxide ring had opened completely or only partially. Preliminary studies [28] showed that upon the addition of the amine curing agent D230 to the GLYMO the system became gel-like after 2 h at room temperature suggesting that the crosslinking has occurred.

Regarding the sol–gel polymerization in GLYMO–D230 system a broad mountain shape band at 1000–1200 cm^{-1} was observed. The major absorption band is actually composed of at least three bands at ~1021 cm^{-1}, ~1055 cm^{-1} and ~1090 cm^{-1}. The band at ~1090 cm^{-1} coincides well with the literature data for POSS derivatives [30] assigned to the stretching vibration of Si–O–Si groups in the silsesquioxane cages (POSS core). A broad band between 3100 and 3600 cm^{-1} and the band at ~1650 cm^{-1} are attributed to OH stretching vibration.

The complex nature of the hybrid system made some peak assignment very difficult and there are a number of "key" overlapping peaks. The presence of PMMA in the hybrid systems is shown by the ester C=O absorption that shifted to higher wave numbers (~1730 cm^{-1}) indicating that intermolecular interactions between PMMA and GLYMO–D230 molecules exists in hybrid systems. The appearance of a weak broad peak around 1540 cm^{-1} is assigned to the combination of the bending vibration of the N–H bond and the stretching vibration of the C–N bond of the amide group, indicating that aminolysis of PMMA occurred. The absorption band at 1000–1200 cm^{-1} assigned to the Si–O–Si stretching vibrations is also observed in all investigated hybrids.

3.2. ^{29}Si CP/MAS NMR spectroscopy

To evaluate the extent of the alkoxysilane hydrolysis–polycondensation reactions in the investigated systems ^{29}Si CP/MAS NMR spectroscopy was used as shown in Fig. 2. For comparison, the spectrum of the polymerized GLYMO (hydrolyzed in acid conditions, cured at 65 °C for 24 h and post-cured at 140 °C for 12 h) is also presented.

In all spectra, the most intense bands are in the region corresponding to T^3 structures (−64 to −68 ppm) while the bands corresponding to T^2 structures (−57 to −61) are hardly seen. There is no clear evidence of T^0 and T^1 species, especially in the spectrum of GLYMO, because of the reduced signal-to-noise ratio. T^0 peak represents silicon atoms with no siloxane linkage and T^1 peak represents silicon atoms with one siloxane bond and two hydroxy (or methoxy) groups, respectively.

The signals at −65.9, −66.9 and −67.5 ppm are in a very good agreement with the literature data [24,25,31] assigned to the fully condensed silsesquioxane T_8 cages. But, in addition to the octahedral structure, the ladder structures are also possible [32]. The chemical shift at about −68.6 can be assigned to decahedra T_{10} [31].

Clear evidence for the ladder structure has not yet been provided. It has been suggested [32,33] that the ladder structures exhibited two bands in IR spectrum due to Si–O bond at 1045–1060 cm^{-1} and 1135–1150 cm^{-1} while the appearance of a single band centered near 1120–1130 cm^{-1} may be taken as good evidence for the presence of a polyhedral structure [32]. In FTIR spectra of our systems a broad mountain shape band of Si–O–Si at 1000–1200 cm^{-1} was observed. A shoulder at ~1055 cm^{-1} could indicate that the polyhedral structures are combined with some ladder-like structures.

3.3. Glass-transition temperature

DSC thermograms showing the glass-transition temperatures, T_gs, of investigated systems are given in Fig. 3.

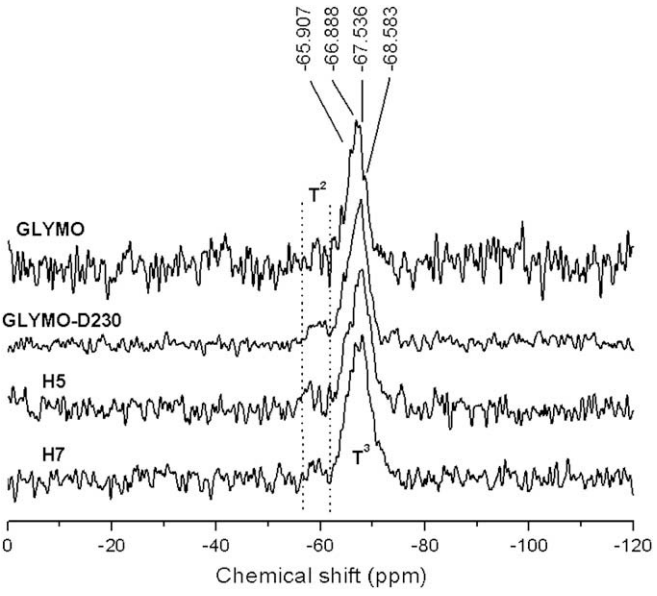

Fig. 2. ^{29}Si NMR spectra of investigated systems.

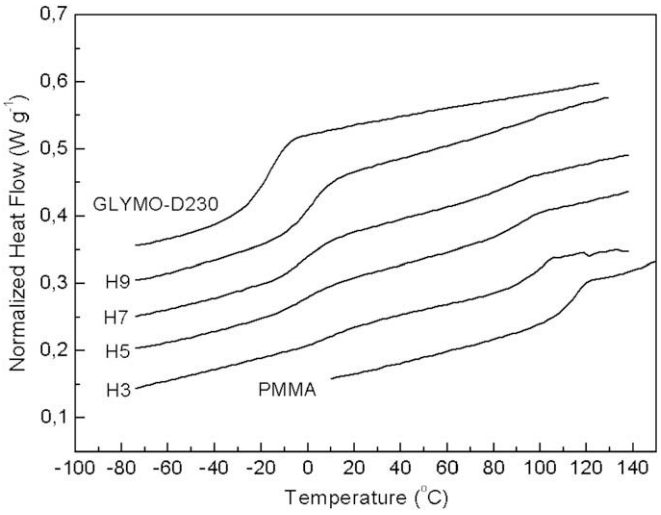

Fig. 3. DSC thermograms of PMMA and hybrid systems.

The glass-transition temperatures of the GLYMO (SSQO)–D230 and PMMA were −17 and 114 °C, respectively (see Table 1). The hybrids showed two T_g values suggesting heterophase morphology (phase-separated systems). An inward shift in T_g values (see ΔT_g[a] column in Table 1) indicated that some extent of interpenetration and/or phase mixing has occurred between GLYMO–D230 structures and PMMA.

Several factors could influence T_g values of hybrid systems. Silsesquioxane structures formed by sol–gel process could reduce the dipole–dipole interactions between PMMA chains (reducing the T_g of PMMA reach phase). If inorganic structures are too big to infiltrate into the free volumes of PMMA, the free volumes of the system increase, the chain segments move more easily and the T_g decrease. On the other side crosslinks hinder the chain-segment motion making the T_g to increase. Intermolecular interactions between silsesquioxane structures and PMMA could also have a positive contribution to the T_g of GLYMO–D230 system.

3.4. Dynamic mechanical analysis

Similar trend in T_g shifts obtained by DSC was observed by means of the dynamic mechanical analysis. Fig. 4 shows the storage modulus (E'), the loss modulus (E'') and the loss factor ($\tan\delta$) as functions of temperature.

Hybrid systems have two distinct E'' and $\tan\delta$ maxima related to the relaxations of the GLYMO–D230 and PMMA in their glass temperature domains. The low-temperature maximum or a shoulder at ca. −80 °C corresponds to the relaxation of the polyoxypropylene chain of the Jeffamine D230 used.

Values of transition temperatures, obtained from the maxima of loss modulus (E''), for the GLYMO–D230 and PMMA enriched phase, $T_{\alpha 1}$ and $T_{\alpha 2}$, are given in Table 1 as well.

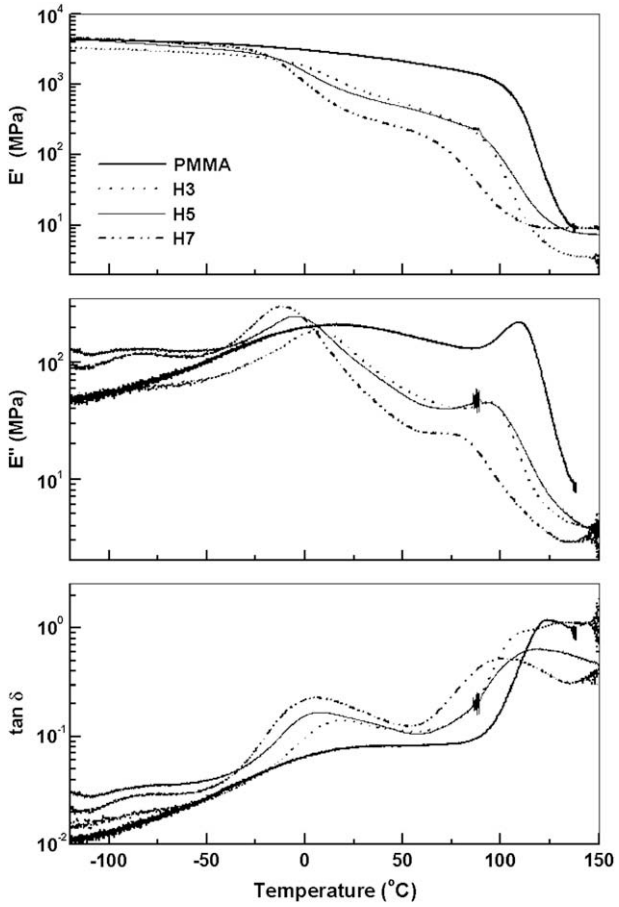

Fig. 4. Dynamic mechanical properties of PMMA and prepared hybrid systems.

Comparing the values of storage modulus above the glass transition of PMMA (rubbery region), at ca. 140 °C, it can be seen that they increase in the order H3 < H5 < H7. It is well documented that the modulus in the rubbery region is related to the crosslink density. For the two-phase systems the presence of a rubbery plateau shows that the structure either consists of a co-continuous morphology with the two phases interpenetrating with one another or of discrete domains dispersed in a continuous crosslinked phase.

From the $\tan\delta$ vs. temperature plot the damping ability of materials can be estimated. According to the literature [34], the $\tan\delta$ values of good damping materials are higher than 0.3 for a temperature range of at least 60 °C. Parameters of the damping ability of investigated systems ($\tan\delta_{max}$ and the temperature range for $\tan\delta > 0.3$, $\Delta T_{\tan\delta>0.3}$) are given in Table 1 as well. For pure PMMA, as for the majority of homopolymers, the temperature range of effective damping is rather narrow and corresponds to an interval of 30 °C in the neighborhood of its glass-transition

Table 1
Transition temperatures, damping ability and solubility of investigated systems.

System	T_g[a]/°C		ΔT_g[a]/°C		T_α[b]/°C		$\tan\delta_{max}$	$\Delta T_{\tan\delta>0.3}$/°C	Gel fraction/%
	T_{g1}	T_{g2}			$T_{\alpha 1}$	$T_{\alpha 2}$			
PMMA		114				109	1.19	106–134	0
H3	12	98	+29	−16	6	94	1.13	>94 (to 146)	81
H5	0	91	+17	−23	−5	89	0.65	>93 (to 178)	84
H7	−2	86	+15	−28	−12	79	0.52	>81 (to 143)	96
GLYMO–D230	−17								82

[a] DSC.
[b] DMA.

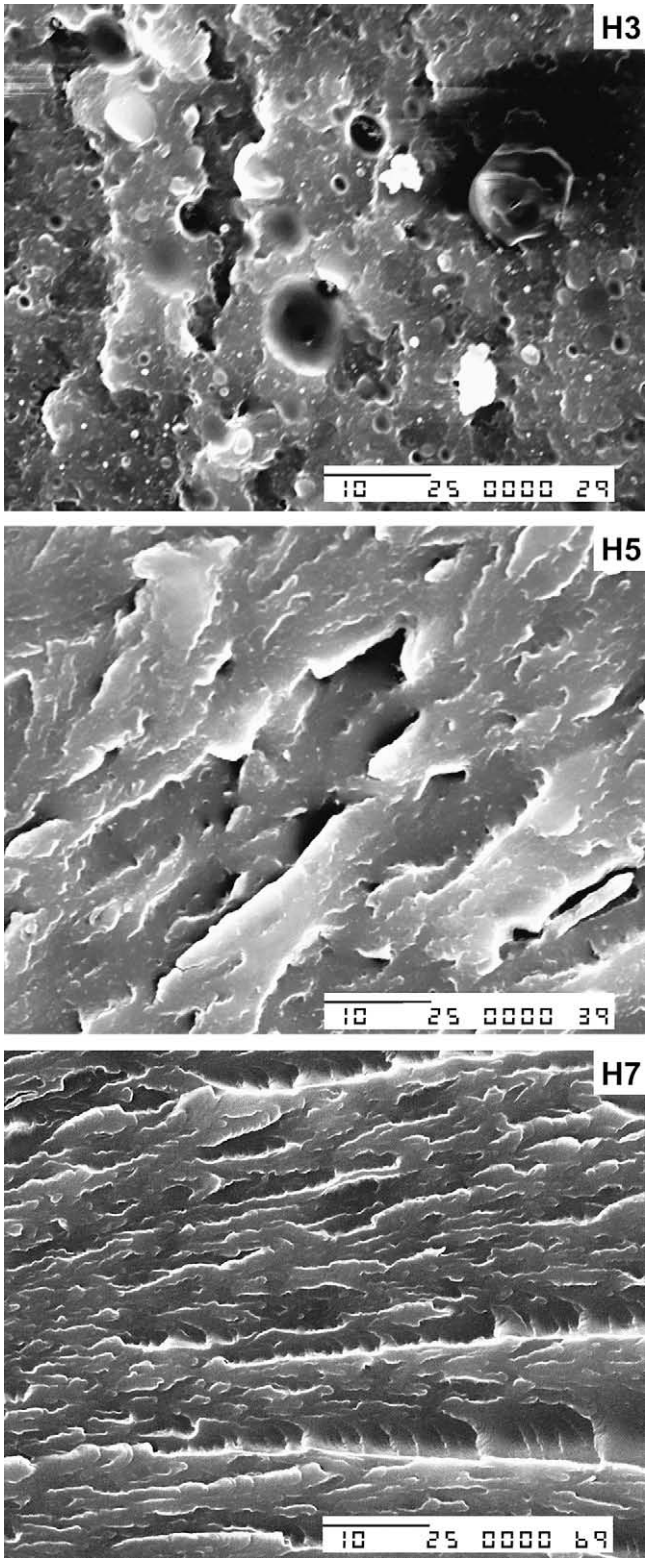

Fig. 5. SEM images of fracture surfaces of hybrid systems. The bars correspond to 10 μm.

temperature. With increasing content of GLYMO–D230 in hybrid systems the relaxation peaks of PMMA enriched phase become wider and lower. tan δ values of hybrids exceed the value 0.3 and, consequently, can show good damping properties, at temperatures higher than 80–90 °C (see Table 1).

3.5. Solvent extraction results

THF extraction results are summarized in Table 1 as well. As expected, THF as a good solvent for the PMMA dissolved it completely. It is worth to note that the gel fraction of GLYMO (SSQO)–D230 system is in a very good agreement with the literature data [35] obtained for an octaepoxy–POSS–D230 network. The possible reactions and network structures obtained from octaepoxy-POSS and amines were studied in detail by Strachota et al. [35]. They found that the networks with higher amine excess ($r > 1$) exhibited significant deviations from a randomly reacted system. The deviations are explained by an unequal reactivity of functional groups (e.g. a lower reactivity of the hydrogen in a secondary amine group with respect to a hydrogen in a primary amine group), by intramolecular reactions and by steric exclusion.

For hybrid system H3 the residual solid content jumped to 80% and continued to increase with increasing inorganic contents. The soluble fraction (between 4 and 19 wt%) is much lower than the nominal content of PMMA in hybrids. These results are in agreement with the data obtained by FTIR spectroscopy indicating that the formation of covalent bonding (crosslinking) between PMMA and D230 chains prevented PMMA from complete dissolving in THF. Crosslinking of PMMA by SSQO–D230 structures is also possible. It is reasonable to suppose that both primary amino groups in D230 are quite independent due to large separation along the chain. Therefore, after the reaction of D230 with silsesquioxane structures the reactivity of the second terminal primary NH_2 group of D230 is not affected. Hence, the reactivity of the NH_2 group in D230 and of the nonreacted primary amino group in SSQO–D230 is the same. However, the kinetics could be affected by a possible microphase separation of SSQO–D230 regions resulting in a nonrandom reaction.

3.6. Hybrid morphology

The SEM images of fracture surfaces (following uniaxial tensile testing) are shown in Fig. 5.

For the hybrid H3 SEM exhibits a heterogeneous morphology in which the minor phase (micrometric phase-separated inorganic domains) forms particles and agglomerates distributed in the continuous matrix. High concentration of voids across the sample surface is the evidence of particle–matrix debonding during deformation. Crack deflection (as in ceramics) is also observed.

Hybrids H5 and H7 have more homogeneous bi-continuous morphology in the micrometric scale indicating better miscibility and interpenetration of networks.

3.7. Surface properties

Results of contact angle measurements of PMMA and hybrid surface with water, formamide and diiodomethane are given in Table 2 together with values of the surface-free energy (γ), its dispersive (γ^d) and polar components (γ^p), estimated using the harmonic mean method proposed by Wu [29].

Table 2
Contact angles (θ), dispersive (γ^d) and polar (γ^p) components of surface-free energy (γ), characterizing the surface of the PMMA and hybrids.

System	$\theta_{H_2O}/^\circ$	$\theta_{HCONH_2}/^\circ$	$\theta_{CH_2I_2}/^\circ$	γ^d/mJ m^{-2}	γ^p/mJ m^{-2}	γ/mJ m^{-2}	γ^p/γ
PMMA	80.0	61.0	27.0	41.6	5.0	46.6	0.11
H3	73.5	61.0	48.0	32.1	10.4	42.5	0.24
H5	65.4	52.3	41.5	34.5	13.7	48.3	0.28
H7	60.0	44.0	38.5	36.4	16.0	52.4	0.31
H9	58.0	51.0	39.5	34.0	16.8	50.8	0.33
GLYMO–D230	58.9	55.0	52.0	29.4	18.2	47.6	0.38

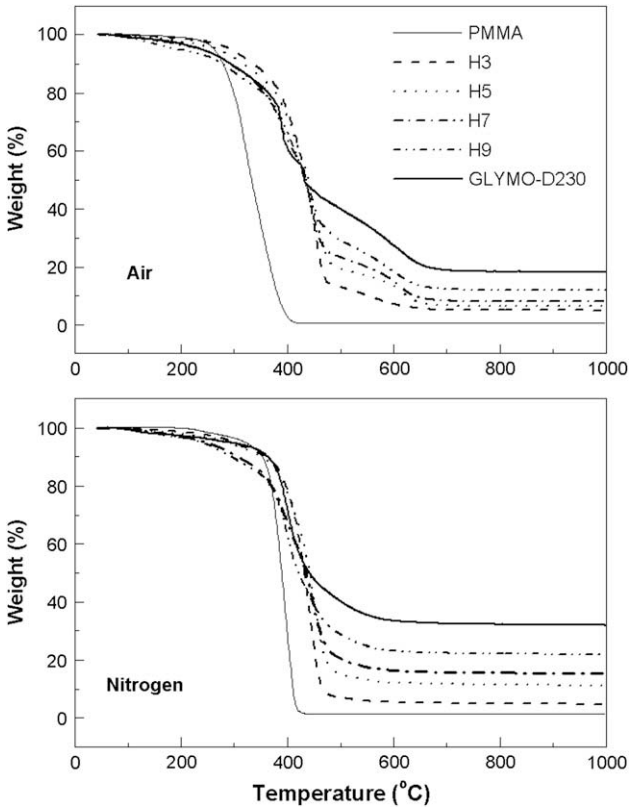

Fig. 6. TGA curves of investigated systems in air and nitrogen.

Water contact angles have been shown to be very sensitive to the nature of the functional groups on the surface. It is necessary to add that all surface imperfections (e.g. adsorbed impurities, microroughness) influence the θ values. PMMA contains both hydrophobic (methylene) and hydrophilic (carbonyl) groups in each unit. The water contact angle decreased from 80° on the pristine PMMA surface to 58° on the H9 surface, indicating the enrichment of hydrophilic groups on the hybrid surface due to the presence of GLYMO–D230 functional groups (such as hydroxyl groups, unreacted amino and epoxy groups) that prevail the water repellency due to the methyl groups of PMMA. In the case of formamide and diiodomethane no evidence for any systematic change in the contact angles was observed. The total surface-free energy of PMMA is close to that of GLYMO–D230 but they differ in the values of the dispersion and polar force contributions.

To estimate the surface polarity, the ratio between the polar force component and the total surface-free energy was calculated (see last column in Table 2). As expected, the polarity increased with increasing content of GLYMO–D230 in hybrid systems improving the water wetting of the surface.

3.8. Thermal decomposition

The TGA results obtained for PMMA, GLYMO–D230 and hybrids under air and nitrogen atmosphere and the first derivative of the TGA (DTG) curves are shown in Figs. 6 and 7.

The TGA and DTG curves of almost all investigated systems (except PMMA and GLYMO–D230 in nitrogen atmosphere) indicate a complex degradation pathway. In fact, at least three to five distinct decomposition stages could be observed. The degradation pathway of PMMA in air is characterized by a broad weight loss in the temperature range 208–422 °C, with the maximum thermal decomposition temperatures at about 378 °C. In radically prepared PMMA two main degradation reactions generally occur. The first, at lower temperature is the depolymerization initiated by the unstable terminal double bonds present in polymer as a consequence of the

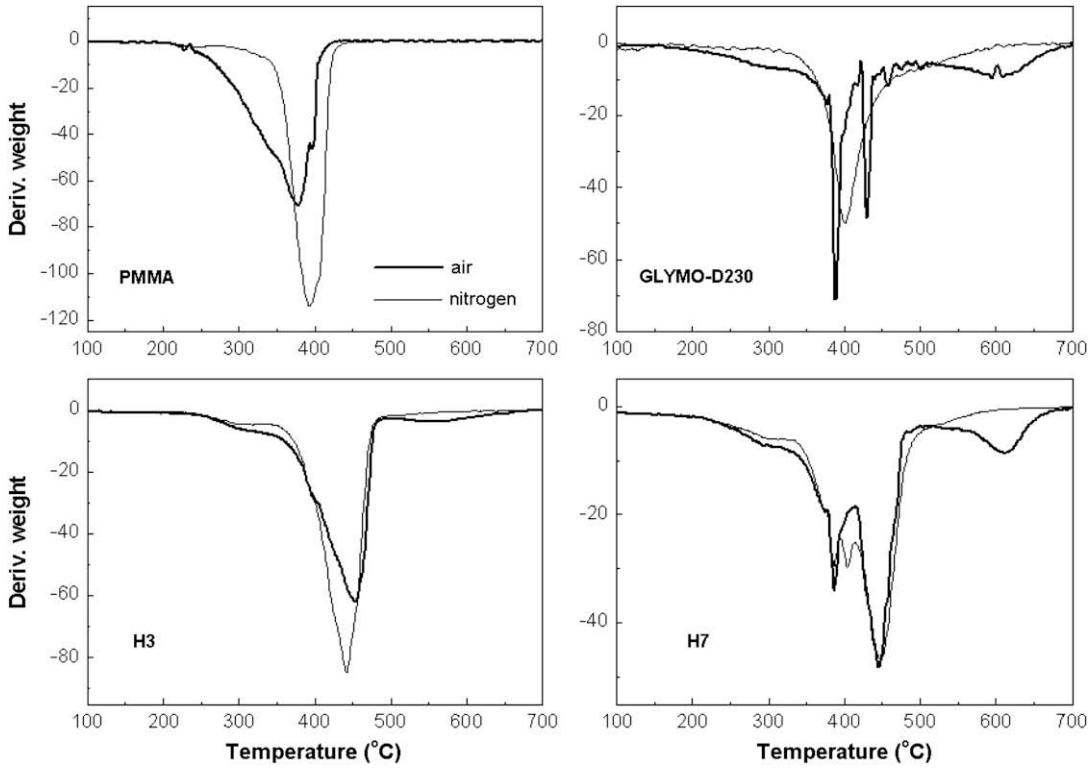

Fig. 7. DTG curves of investigated systems in air and nitrogen.

disproportionate termination reaction while the second is the random degradation of the polymer chains.

The DTG curve of the GLYMO–D230 in air is characterized with a shoulder centered at 283 °C, two other degradation steps peaking at 390 and 429 °C and with a broad high temperature peak centered at ca. 616 °C.

Degradation of epoxy–amine systems has been widely studied due to their widespread use as engineering polymers. It was determined that it proceeds via three overlapping mechanisms. The first, starting already at 240 °C, consists of homolytic scission of chemical bonds in the network, which influences its physical properties but does not cause a large weight loss [36,37]. The first major weight loss in both oxidative and non-oxidative degradation of amine cured epoxies is caused by dehydration due to elimination of water molecule from the oxypropylene group, $-CH_2-CH(OH)-$, and subsequent formation of double bonds. This dehydration is concurrent with network breakdown [36,38,39]. The final degradation proceeds through reactions of isomerisation, intramolecular cyclisation, chain transfer and other reactions that involve the radicals formed in the initial stages of degradation [38].

The degradation of PMMA in nitrogen can be described by a single step in the temperature range 330–440 °C with the maximum thermal decomposition temperature at 394 °C. For GLYMO–D230 the temperature of maximum rate of weight loss in nitrogen is 402 °C and the DTG peak has a shoulder between 440 and 600 °C.

In hybrid systems the oxidative atmosphere seems not to have marked effect on thermal degradation. As seen from Fig. 7 the thermal decomposition behaviors of hybrids in air are close to those in nitrogen except for the appearance of a decomposition peak in DTG curve at higher temperature (520–690 °C), which might attribute to the thermal decomposition of polymer chains trapped in inorganic network. The data shown in Fig. 6 also confirm this assumption because the char residuals in air are less than those in nitrogen.

In comparison to the neat PMMA the main decomposition of hybrids shifted to higher temperature (for 50–60 °C in nitrogen and for 70–80 °C in air, respectively).

The higher thermal stability of hybrids may be due to the inorganic structures formed by sol–gel process that can probably restrain the attack of the free radicals. The interpenetration of polymer networks can also reduce the movement of free radicals and their attack on PMMA main chain to cause chain scission.

4. Conclusions

New organic–inorganic hybrids based on poly(methyl methacrylate) and silsesquioxane structures were prepared by *in situ* bulk polymerization. The inorganic phase was generated from 3-glycidyloxypropyltrimethoxysilane (GLYMO) via sol–gel chemistry. Poly (oxypropylene)diamine was used as an epoxy opening agent, as basic catalyst for GLYMO condensation and as PMMA crosslinking agent. Chemical reactions in the systems of different MMA/GLYMO molar ratio were studied by Fourier transform infrared analysis. The high degree of conversion of methoxysilyl groups to –Si–O–Si– linkages was confirmed by ^{29}Si NMR. Hybrid morphology was studied by SEM. Hybrid with ca. 3% of inorganic phase (calculated as $SiO_{1.5}$) showed a discrete microstructure while hybrids with higher amount of inorganic phase (ca. 5 and 7%) showed characteristic IPN morphology. Silsesquioxane structures formed as a result of GLYMO hydrolysis and condensation in the sol–gel process influence the glass-transition temperature of PMMA. The hybrids have much better thermal stability than PMMA and showed excellent solvent (THF) resistance. Their surfaces are more hydrophilic than PMMA and they may have potential as damping materials.

Acknowledgments

This study is a part of the research project: "Bioceramic, Polymer and Composite Nanostructured Materials", 125-1252970-3005, supported by the Ministry of Science, Education and Sports in the Republic of Croatia. The authors are grateful for this support.

References

[1] Schubert U, Hüsing N, Lorenz A. Chem Mater 1995;7(11):2010–27.
[2] Matejka L, Dusek K, Plestil J, Kriz J, Lednicky F. Polymer 1999;40(1):171–81.
[3] Novak BM. Adv Mater 1993;5(6):422–33.
[4] Girardreydet E, Lam TM, Pascault JP. Macromol Chem Phys 1994;195(1):149–58.
[5] Wen JA, Mark JE. J Appl Polym Sci 1995;58(7):1135–45.
[6] Jackson CL, Bauer BJ, Nakatani AI, Barnes JD. Chem Mater 1996;8(3):727–33.
[7] Mark JE. Polymer 1997;38(17):4523–9.
[8] Mccarthy DW, Mark JE, Schaefer DW. J Polym Sci Part B Polym Phys 1998; 36(7):1167–89.
[9] Matejka L, Dukh O, Kolarik J. Polymer 2000;41(4):1449–59.
[10] Zhou W, Mark JE, Unroe MR, Arnold FE. J Appl Polym Sci 2001;79(13):2326–30.
[11] Chen WC, Lee SJ. Polym J 2000;32(1):67–72.
[12] Palkovits R, Althues H, Rumplecker A, Tesche B, Dreier A, Holle U, et al. Langmuir 2005;21(13):6048–53.
[13] Mammeri F, Le Bourhis E, Rozes L, Sanchez C. J Eur Ceram Soc 2006;26(3):259–66.
[14] Avila-Herrera CA, Gomez-Guzman O, Almaral-Sanchez JL, Yanez-Limon JM, Munoz-Saldana J, Ramirez-Bon R. J Non-Cryst Solids 2006;352(32–35):3561–6.
[15] Yeh JM, Hsieh CF, Yeh CW, Wu MJ, Yang HC. Polym Int 2007;56(3):343–9.
[16] Sun JJ, Akdogan EK, Klein LC, Safari A. J Non-Cryst Solids 2007;353(29):2807–12.
[17] Shimomura J, Ogihara T, Ogata N, Kozuka H, Kato K, Suzuki H. J Ceram Soc Jpn 2007;115(1345):556–61.
[18] Kopesky ET, Haddad TS, Cohen RE, McKinley GH. Macromolecules 2004; 37(24):8992–9004.
[19] Kopesky ET, Haddad TS, McKinley GH, Cohen RE. Polymer 2005;46(13):4743–52.
[20] Kopesky ET, McKinley GH, Cohen RE. Polymer 2006;47(1):299–309.
[21] Amir N, Levina A, Silverstein MS. J Polym Sci Part A Polym Chem 2007; 45(18):4264–75.
[22] Xu HY, Yang BH, Wang JF, Guang S, Li C. J Polym Sci Part A Polym Chem 2007; 45(22):5308–17.
[23] Kotal A, Si S, Paira TK, Mandal TK. J Polym Sci Part A Polym Chem 2008; 46(3):1111–23.
[24] Matejka L, Dukh O, Brus J, Simonsick WJ, Meissner B. J Non-Cryst Solids 2000; 270(1–3):34–47.
[25] Matejka L, Dukh O, Hlavatá D, Meissner B, Brus J. Macromolecules 2001; 34(20):6904–14.
[26] Pavlinec J, Lazar M. J Appl Polym Sci 1995;55(1):39–45.
[27] Pavlinec J, Lazar M, Janigova I. J Macromol Sci Pure Appl Chem 1997; A34(1):81–90.
[28] Vrabec T. Diploma thesis, Fac Chem Eng Technol, University of Zagreb, Zagreb; 2007 [in Croatian].
[29] Wu S. J Polym Sci Part C 1971;34:19–30.
[30] Sheen YC, Lu CH, Huang CF, Kuo SW, Chang FC. Polymer 2008;49(18):4017–24.
[31] Romeo HE, Fanovich MA, Williams RJJ, Matejka L, Plestil J, Brus J. Macromolecules 2007;40(5):1435–43.
[32] Brown JF, Vogt LH, Prescott PI. J Am Chem Soc 1964;86(6):1120.
[33] Baney RH, Itoh M, Sakakibara A, Suzuki T. Chem Rev 1995;95(5):1409–30.
[34] Babkina NV, Lipatov YS, Alekseeva TT. Mech Comp Mater 2006;42(4):385–92.
[35] Strachota A, Whelan P, Kriz J, Brus J, Urbanova M, Slouf M, et al. Polymer 2007;48(11):3041–58.
[36] Patterson-Jones JC, Smith DA. J Appl Polym Sci 1968;12(7):1601–20.
[37] Zakordonskiy VP, Hnatyshin SY, Soltys MM. Polym J Chem 1998;72(12):2610–20.
[38] Patterson-Jones JC. J Appl Polym Sci 1975;19(6):1539–47.
[39] Grassie N, Guy MI, Tennent NH. Polym Degrad Stab 1986;14(2):125–37.